arXiv:0803.1140v1 [cond-mat.mes-hall] 7 Mar 2008

Incompressible Liquid, Stripes and Bubbles in rapidly rotating Bose atoms at $\nu = 1$

Hidetsugu Seki and Kazusumi Ino
Department of Pure and Applied Science, University of Tokyo,
Komaba 3-8-1, Meguro-ku, Tokyo, 153-8902, Japan

We numerically study the system of rapidly rotating Bose atoms at the filling factor (ratio of particle number to vortex number) $\nu = 1$ with the dipolar interaction. A moderate dipolar interaction stabilizes the incompressible quantum liquid at $\nu = 1$. Further addition induces a collapse of it. The state after the collapse is a compressible state which has phases with stripes and bubbles. There are two types of bubbles with a different array. We also investigate models constructed from truncated interactions and the models with the three-body contact interaction. They also have phases with stripes and bubbles.

PACS numbers: 03.75.Lm,03.75.Kk,73.43.Nq

I. INTRODUCTION

Recently rapidly rotating ultracold atoms in a trap have attracted considerable interest. Experimental studies of moderately rotating atomic Bose gases have shown evidence for the formation of a vortex lattice[1,2]. Bose-Einstein condensation occurs even in the case without interaction but it is interaction which forms a vortex lattice. The number which parameterizes the population of vortices is given by $\nu = N/N_V$ where N is the number of bosons and N_V is the average number of vortices. For $\nu > \nu^*$ where $\nu^* \sim 6$, the vortex lattice is stable[3]. For the high frequency regime $\nu < \nu^*$, numerical studies have predicted that the vortex lattice ought to melt and should be replaced by incompressible liquids which are closely related to fractional quantum Hall states[3,4,5]. In that regime, ν corresponds to the filling of the Landau levels in the rotating plane. At $\nu = 1/2$, the bosonic Laughlin state[6] is predicted[5], while at $\nu = k/2$ (k is an integer ≥ 2), states with a clustered structure emerge[3]. For $k = 2$ it is called the Pfaffian state[7]. Its fermionic counterpart is believed to be realized in the $\nu = 5/2$ plateau[8] and has been proposed as an excellent candidate for a quantum computational device[9].

In typical Bose atomic gases, the interaction is short-ranged and can be modeled by a contact interaction[10]. Recently the condensation of Bose atoms with a strong magnetic dipole moment has been observed[11]. These atoms interact nonlocally through the dipolar interaction. The effect of the dipolar interaction on vortex lattices and incompressible liquids above has been studied for $\nu = 1/2$[12], $\nu = 3/2$[13] and $\nu = 2$[14]. For these cases, a moderate dipolar interaction stabilizes the incompressible liquids. When the dipolar interaction gets strong, however, these states collapse. For the $\nu = 1/2$ case, the state after the collapse is identified as a stripe state in both Gross-Pitaevskii mean-field theory and microscopic theory[12]. As the dipolar interaction gets strong, the stripe state at $\nu = 1/2$ eventually shows a transition to a bubble state[12]. Similar transitions are also observed for $\nu = 2$[14]. A tendency of a spectrum to form stripes is mentioned also for $\nu = 3/2$[13]. These stripes and bubbles are closely related to those of two-dimensional fermions in higher Laudau levels[21,22,23].

In this paper, we consider the finite system of Bose atoms at $\nu = 1$ (up to $N = 12$) which interact through the dipolar interaction and perform an exact diagonalization study to examine whether similar stabilization and collapse are induced. We observe the stabilization of the Pfaffian state similar to those of incompressible liquids at $\nu = 1/2, 3/2$ by a moderate dipolar interaction. Further addition of the dipole moment induces a collapse of the incompressible liquid. To investigate the nature of the collapse, we take the periodic rectangular geometry. This geometry is suitable to address bulk properties and transitions to other states. For the cases we have investigated up to $N = 12$, we observe four types of states: stripes, bubbles, intermediate states of two types of stripes, and intermediate states of stripes and bubbles. These states are compressible and therefore sensitive to geometry. The periodic rectangular geometry is parameterized by an aspect ratio (≤ 1). We study the spectral flow of low-lying levels due to the change of the aspect ratio in detail. We also use the pair distribution function and the guiding-center static structure factor of ground states. They give a consistent picture of phases of the $\nu = 1$ Bose atoms. For the stripe states, the direction and the number of stripes depend on the aspect ratio and the interaction. For large aspect ratios, we observe that the increase of the strength of the dipolar interaction results in the formation of bubbles. Further addition of the dipolar interaction leads to a transition to another bubble state which has a different array. For small aspect ratios, stripe states seem to be favored even when the strength of the dipolar interaction is strong : we observe no evidence that a transition from stripes to bubbles occurs.

To elucidate the nature of these transitions and realized states, we consider models constructed from truncated interactions. Any two-body interaction between particles in the lowest Landau level can be expanded in pseudopotential[15] $V_m, m = 0, 1, 2, 3, \cdots$, each term of which corresponds to the projection to the two particle states with definite relative angular momentum. For bosons, the odd terms vanish $V_m = 0, m = 1, 3, 5, \cdots$.

For the dipolar interaction, all the even terms $V_m, m = 0, 2, 4, \cdots$ appear. We investigate the model only with the V_2 interaction ("hollow-core"). It turns out that this model is always in a bubble phase for the aspect ratio above ~ 0.5. A certain amount of the two-body contact interaction V_0 causes a transition to another bubble state with a different array. For small aspect ratios below ~ 0.5, we observe the formation of stripes.

These results are for two-body interactions. We also address the same issue to the three-body contact interaction, for which the Pfaffian state is the exact ground state[16]. We investigate the effect of the V_2 interaction on the model. Similar transitions to stripes and bubbles are observed also for this model.

The organization of this paper is as follows. In Sec. II, we give details of the formalism used to treat the bose problem on the periodic rectangular geometry. In Sec. III, we show results for the dipolar model. In Sec.IV is devoted to the V_2 model. In Sec.V, we show results for the three-body contact interaction. Sec.VI gives conclusions.

II. FORMALISM

The Hamiltonian describing N bosons of mass m in a rotating coordinate is

$$\begin{aligned} H &= \sum_{i=1}^{N} \frac{1}{2m}(\mathbf{p}_i - m\omega\hat{\mathbf{z}}\times\mathbf{r}_i)^2 \\ &\quad + \sum_{i=1}^{N}\frac{1}{2}m(\omega_0^2-\omega^2)(x_i^2+y_i^2) + \sum_{i=1}^{N}\frac{1}{2}m\omega_z^2 z_i^2 \\ &\quad + \sum_{1\le i<j\le N} V(\mathbf{r}_i-\mathbf{r}_j), \end{aligned} \tag{1}$$

where the angular velocity is $\omega\hat{\mathbf{z}}$, the x-y trap frequency is ω_0, and the axial trap frequency is ω_z. The confinement length in the rotating plane (the x-y plane) is $l \equiv \sqrt{\hbar/(m\omega_0)}$ and the confinement length along the z-direction is $l_z \equiv \sqrt{\hbar/(m\omega_z)}$. When ω_z is sufficiently large, the strong confinement along the z-direction freezes the motion along the z-direction in the ground state of the harmonic oscillator and the motion becomes quasi two-dimensional. For $\omega \sim \omega_0$, the system is equivalent to the bosons of charge q in a magnetic field $\mathbf{B} = (2m\omega/q)\hat{\mathbf{z}}$. When ω is sufficiently large and interaction is weak, we can treat the x-y motion to be restricted to the lowest Landau level. For N bosons spread over an area A, the characteristic parameter is $\nu \equiv N/N_V$ where $N_V = (m\omega A)/\pi\hbar$ is the average number of vortices. In this paper, we focus our attention at $\nu = 1$.

Let us next describe interactions between the atoms. The two-body contact interaction[10] is given by

$$V_0 = g \sum_{1\le i<j\le N} \delta^3(\mathbf{r}_i-\mathbf{r}_j), \tag{2}$$

where $g = 4\pi\hbar^2 a_s/m$ (a_s is the s-wave scattering length). In typical Bose atoms, the interaction between particles is short-ranged and can be approximated excellently by V_0. Next, the electric or magnetic dipole interaction is given by

$$V_{\rm dip} = C_d \sum_{1\le i<j\le N} \frac{\mathbf{p}_i\cdot\mathbf{p}_j - 3(\mathbf{n}_{ij}\cdot\mathbf{p}_i)(\mathbf{n}_{ij}\cdot\mathbf{p}_j)}{|\mathbf{r}_i-\mathbf{r}_j|^3}, \tag{3}$$

where $\mathbf{n}_{ij} = (\mathbf{r}_i-\mathbf{r}_j)/|\mathbf{r}_i-\mathbf{r}_j|$, the $\mathbf{p}_i' s$ are unit vectors which represent direction of the dipole moment. We assume that the dipole moments are parallel to the z-direction. The model with the dipolar interaction $H = V_0 + V_{\rm dip}$ will be called as the dipolar model below. We expand H in pseudopotential[15] $V_m, m = 0, 1, 2, \cdots$. For bosons, only even m contribute. V_m depends on the trap asymmetry l_z/l. We assume that ω_z is sufficiently large compared to ω so that we can take the limit that the thickness along the z-direction of the two-dimensional motion (in the xy plane) is negligible, $l_z/l \to 0$. To first order in l_z/l, the pseudopotential is given by[12]

$$V_0 = \sqrt{\frac{2}{\pi}}\frac{\hbar^2 a_s}{ml^2 l_z} + \sqrt{\frac{2}{\pi}}\frac{C_d}{l^2 l_z} - \sqrt{\frac{\pi}{2}}\frac{C_d}{l^3} \tag{4}$$

$$V_{m>0} = \sqrt{\frac{\pi}{2}}\frac{(2m-3)!!}{m!2^m}\frac{C_d}{l^3} \tag{5}$$

The strength of the dipolar interaction in the dipolar model $V_0 + V_{\rm dip}$ is controlled by $\alpha \equiv V_2/V_0$. We will also denote the potential with $V_k \neq 0$ for $k = i$, $V_k = 0$ for $k \neq i$ as V_i below.

For realistic atoms, there are higher order terms of many-body interactions. The first of them is the three-body contact interaction

$$V_{\rm 3b} = C_{3b} \sum_{1\le i<j<k\le N} \delta^3(\mathbf{r}_i-\mathbf{r}_j)\delta^3(\mathbf{r}_i-\mathbf{r}_k). \tag{6}$$

The exact zero-energy ground state of $V_{\rm 3b}$ is the Pfaffian state[16] : for the disk geometry in the symmetric gauge, it is given by (except for the gaussian factor of the lowest Landau level)

$$\Psi_{\rm Pf} = {\rm Pf}\left(\frac{1}{Z_i - Z_j}\right)\prod_{i<j}(Z_i - Z_j) \tag{7}$$

where $Z_i = x_i + iy_i$. This state is expected to have quasiparticles and quasiholes with nonabelian statistics[7]. The modular S matrices underlying the statistics have been studied in Ref.[17].

We consider several models with these interactions on the periodic rectangular geometry. We denote the sides of the rectangular as a and b. The translational invariance of the system gives a conserved pseudomomentum[18] $\mathbf{K} = (K_x, K_y)$. The pseudomomentum runs over a Brillouin zone containing $\bar{N}^2$ points, where $\bar{N}$ is the greatest common division of N and N_V. K_x, K_y is measured in units of $2\pi\hbar/a$ and $2\pi\hbar/b$ respectively. The states at $(\pm K_x, \pm K_y)$ are degenerate by symmetry so we may take only positive K_x, K_y.

Next we recall the definition of some functions. The guiding-center static structure factor $S_0(\mathbf{q})$ for a state $|\Psi\rangle$ is given by

$$S_0(\mathbf{q}) = \sum_{i,j} \langle\Psi| \, e^{i\mathbf{q}\cdot(\mathbf{R}_i - \mathbf{R}_j)} \, |\Psi\rangle \,, \tag{8}$$

where $\mathbf{R}_i$ is the guiding center of the i-th particle(See Ref.[24] for detail). Also, the pair distribution function in the real space $G(\mathbf{r})$ is defined by

$$G(\mathbf{r}) = \frac{ab}{N(N-1)} \langle\Psi| \sum_{i \neq j} \delta(\mathbf{r} - \mathbf{r}_i - \mathbf{r}_j) |\Psi\rangle \tag{9}$$

$G(\mathbf{r})$ and $S_0(\mathbf{q})$ will be used to study the nature of ground states.

III. RESULTS FOR THE DIPOLAR MODEL

In this section, we present results of exact diagonalizations of the dipolar model $V_0 + V_{\rm dip}$ at $\nu = 1$. The strength of the dipolar interaction is controlled by α defined in the previous section. As discussed in Ref.[3], the ground state at $\alpha = 0$ is an incompressible liquid and has a large overlap with the Pfaffian state. We add a moderate dipolar interaction (small α) and examine the stability of the incompressible liquid.

We first fix the aspect ratio to be 1.0. For even N up to 12, we observe that three nearly degenerate states with lowest energies appear at $\mathbf{K}$ where the Pfaffian states exist and are clearly separated from the rest of the spectrum.

In Fig. 1, we present the squared overlaps of two degenerate ground states and a nearly degenerate state with the Pfaffian states for $N = 10$ as functions of α. At small α, the overlaps increase monotonically as α increases. The maximum of the overlaps is reached around $\alpha \sim 0.3$. Thus a moderate dipolar interaction with α below 0.3 stabilizes the Pfaffian states. Figure 2 shows the pair distribution function $G(\mathbf{r})$ of the Pfaffian state for $N = 10$ and the ground state of the dipolar model for $N = 12$ at $\alpha = 0.3$. Both states have very similar shapes of $G(\mathbf{r})$. Except for regions near four corners on the rectangular boundary, $G(\mathbf{r})$ is almost constant and isotropic. This property indicates incompressibility of the Pfaffian state. The $G(\mathbf{r})$ of the ground state of the dipole model for $N = 12$ is slightly flatter than that of the Pfaffian state for $N = 10$. The nearly degenerate states in two other sectors of $\mathbf{K}$ have similar $G(\mathbf{r})$.

When the dipolar interaction gets strong, the overlaps show a very abrupt drop. It occurs around $\alpha \sim 0.4$ for all the sectors as shown in Fig. 1. We observe similar stabilization and collapse occur in the region $a/b = 0.3 \sim 1.0$. The strength of the dipolar interaction α^* where the collapse occurs vary with the aspect ratio. If we decrease the aspect ratio, α^* gradually increases and reaches to ~ 0.5 at $a/b = 0.3$. We also confirm that similar stabilization and collapse occur for $N = 6, 8$ at $\alpha = 0.4 \sim 0.5$ for $a/b = 0.3 \sim 1.0$.

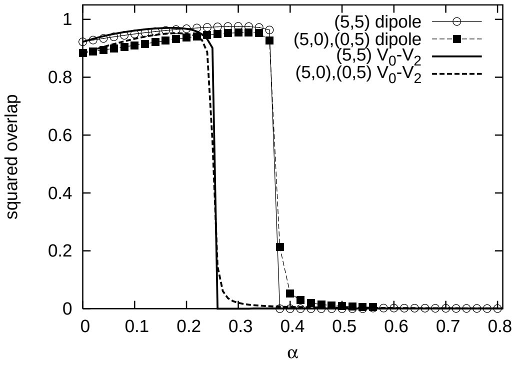

FIG. 1: The squared overlaps of the two degenerate ground states and a nearly degenerate state for both the dipolar and the $V_0 - V_2$ model with the Pfaffian states are shown for $N = 10$ at $a/b = 1.0$. The Pfaffian states exist at $\mathbf{K} = (5,5), (5,0), (0,5)$. The two degenerate ground states appear at $\mathbf{K} = (5,0), (0,5)$. The degeneracy is due to geometrical symmetry at $a/b = 1.0$.

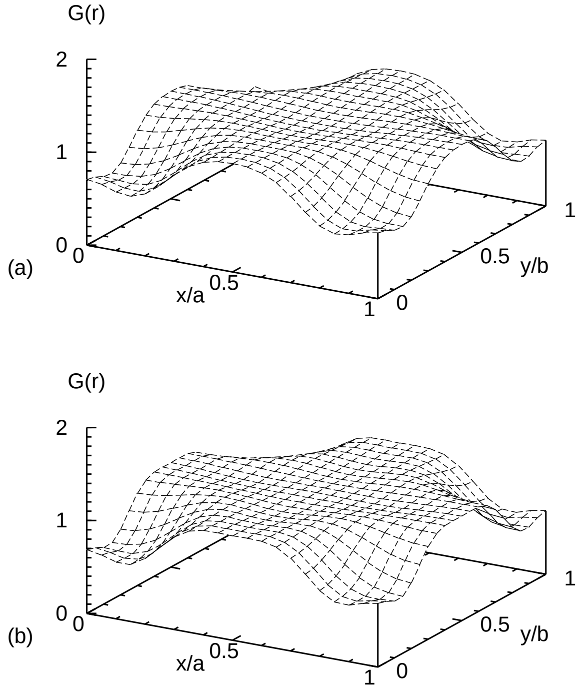

FIG. 2: Pair distribution function $G(\mathbf{r})$ of various states at $a/b = 1.0$. (a) The Pfaffian state for $N = 10$ at $\mathbf{K} = (0,5)$. (b) The ground state of the dipolar model for $N = 12$ at $\alpha = 0.30, \mathbf{K} = (6,6)$.

We next investigate states after the collapse of the incompressible liquid. In Fig. 3, we present the energy spectrum for $N = 10$ at $\alpha = 0.65$ and $a/b = 0.8$. The

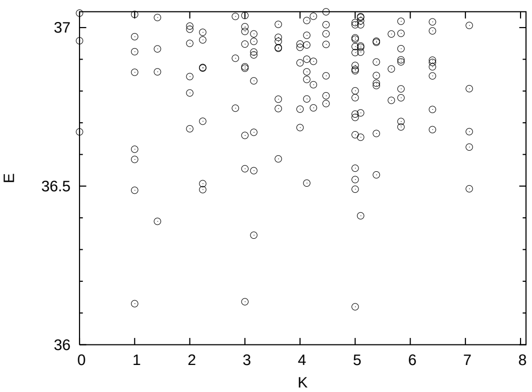

FIG. 3: Energy spectrum of the dipolar model for $N = 10$ at $\alpha = 0.65, a/b = 0.8$ as a function of $K = \sqrt{K_x^2 + K_y^2}$. The ground state at $\mathbf{K} = (0, 5)$ and states at $\mathbf{K} = (0, 3), (0, 1)$ are quasidegenerate.

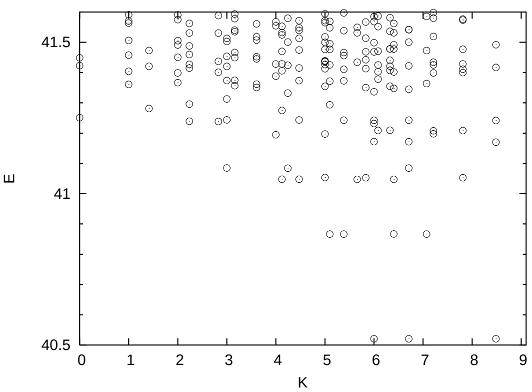

FIG. 5: Energy spectrum of the dipolar model for $N = 12$ at $\alpha = 0.6, a/b = 0.5$. The ground state at $\mathbf{K} = (6, 0)$ and states at $\mathbf{K} = (6, 3), (6, 6)$ are quasidegenerate. The lowest energy states at $\mathbf{K} = (5, 1), (5, 2), (5, 4), (5, 5)$ form a quasidegenerate first-excited states.

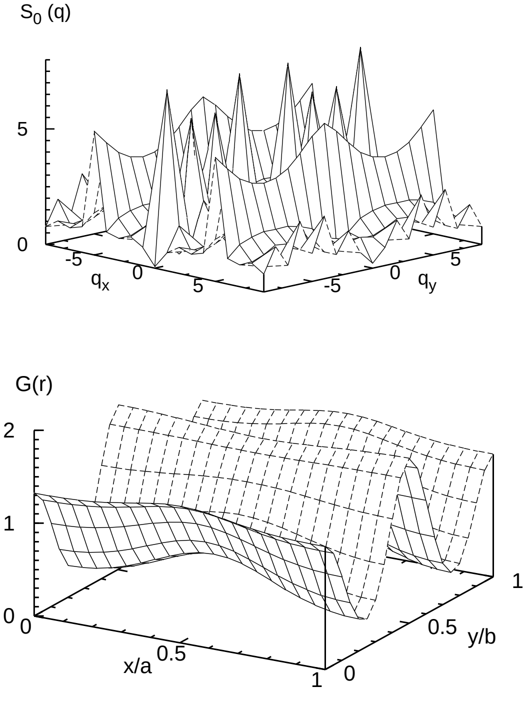

FIG. 4: Guiding-center static structure factor $S_0(\mathbf{q})$ and pair distribution function $G(\mathbf{r})$ of the ground state of the dipolar model for $N = 10$ at $\alpha = 0.65, a/b = 0.8, \mathbf{K} = (0, 5)$.

ground state at $\mathbf{K} = (0, 5)$ and the lowest energy states at $\mathbf{K} = (0, 3), (0, 1)$ are quasidegenerate and clearly separated from the rest of the spectrum. A characteristic wave vector that separates these quasidegenerate states is $\mathbf{K}^* = (0, 2)$. This suggests that these quasidegenerate ground states have a tendency to form a stripe state.

Let N_D be the number of distinct quasidegenerate ground states, and let N_s be the number of stripe. There are $\bar{N}^2$ distinct values in the Brillouin zone, where $\bar{N}$ is the greatest common divisor of N and N_V. If the translational symmetry is broken in one direction, the length of the Brillouin zone of the one-dimensional superlattice is $(2\pi\bar{N})/(LN_D)$ where L is the period of the superlattice. It must be $2\pi/(L/N_s)$ where L/N_s is the length per stripe. This yields $N_sN_D = \bar{N}$. For $\nu = 1$,$\bar{N} = N$. The relation $N_sN_D = N$ yields the number of boson per stripe $M = N/N_s = N_D$. In the case above, $N = 10$ and $N_D = 5$, which gives $N_s = 2$ and $M = 5$.

To study properties of these quasidegenerate states, we calculate the guiding-center static structure factor $S_0(\mathbf{q})$ and the pair distribution function $G(\mathbf{r})$ of the ground state. We measure q_x and q_y in units of $2\pi\hbar/a$ and $2\pi\hbar/b$. In Fig. 4, we present $S_0(\mathbf{q})$ of the ground state for $N = 10$ at $\alpha = 0.65$, $a/b = 0.8, \mathbf{K} = (0, 5)$. There are peaks at $\pm\mathbf{q}^* = (0, \pm 2)$ and $\pm 2\mathbf{q}^*$. Other peaks at $\pm 3\mathbf{q}^*, \pm 4\mathbf{q}^*$ are due to the translational symmetry at $\nu = 1$. The peaks at $\pm\mathbf{q}^* = (0, \pm 2)$ indicate a strong density-density correlation in the ground state at this ordering vector. In Fig. 4, we also present $G(\mathbf{r})$ of the state. The shape of $G(\mathbf{r})$ is quite different from that of the Pfaffian state shown in Fig. 2. $G(\mathbf{r})$ depends on the y-direction but has little dependence along the x-direction. Two peaks are seen along the y-direction in the unit cell, which is consistent with the peak of $S_0(\mathbf{q})$ at $\mathbf{q}^* = (0, 2)$. $S_0(\mathbf{q})$ and $G(\mathbf{r})$ indicate that this ground state is a stripe state with two stripes lying parallel to the x-direction. This is consistent with the analysis of N_s given in the previous paragraph. $S_0(\mathbf{q})$ and $G(\mathbf{r})$ of other quasidegenerate states at $\mathbf{K} = (0, 3), (0, 1)$ are similar to those of the ground state at $\mathbf{K} = (0, 5)$.

In Fig. 5, we present the energy spectrum for $N = 12$ at $\alpha = 0.6$, $a/b = 0.5$. The ground state at $\mathbf{K} = (6, 0)$ and the lowest energy state at $\mathbf{K} = (6, 3), (6, 6)$ are quasidegenerate and clearly separated from the rest of the spectrum. These states are separated by a characteristic wave vector $\mathbf{K}^* = (0, 3)$. The direction of stripes is parallel to the x-direction and the number of stripes

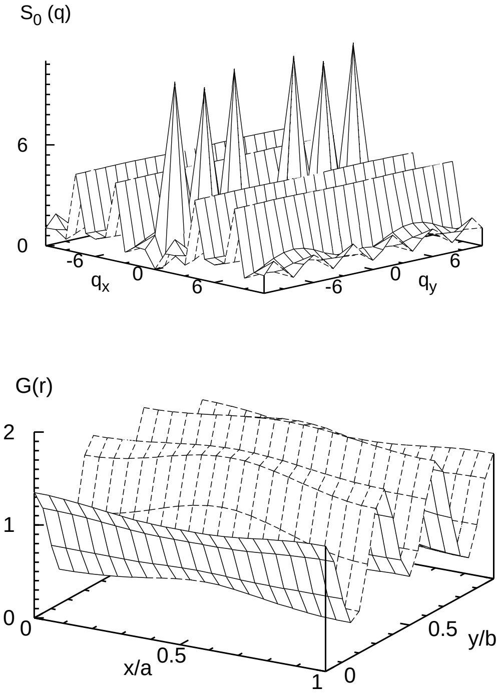

FIG. 6: $S_0(\mathbf{q})$ and $G(\mathbf{r})$ of the ground state of the dipolar model for $N = 12$ at $\alpha = 0.6, a/b = 0.5, \mathbf{K} = (6, 0)$.

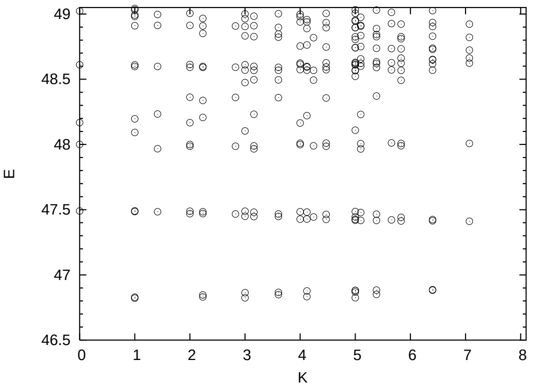

FIG. 7: Energy spectrum of the dipolar model for $N = 10$ at $\alpha = 1.0, a/b = 0.8$. The quasidegenerate states are at $\mathbf{K}$ =(1,0),(0,1),(2,1),(1,2)(3,0),(0,3),(2,3),(3,2) ,(4,1),(1,4),(4,3),(3,4),(5,0),(0,5),(4,5),(5,4),(2,5),(5,2).

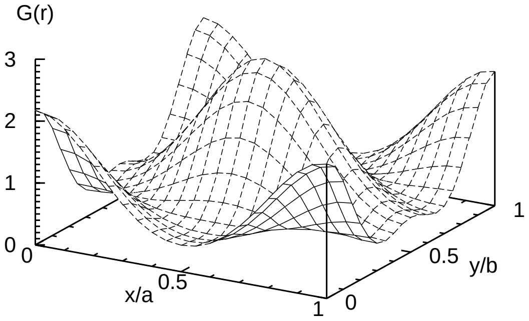

FIG. 8: $G(\mathbf{r})$ of the ground state of the dipolar model for $N = 10$ at $\alpha = 1.0, a/b = 0.8, \mathbf{K} = (0, 5)$.

is three. Fig. 6 shows $S_0(\mathbf{q})$ and $G(\mathbf{r})$ of the ground state. There are peaks at $\pm\mathbf{q}^* = (0, \pm 3)$ and at $\pm 2\mathbf{q}^*$. Other peaks at $\pm 3\mathbf{q}^*$ are due to the translational symmetry. We also present $G(\mathbf{r})$ of the ground state in Fig. 6. There are three peaks along the y-direction. This is consistent with the peak of $S_0(\mathbf{q})$ at $\mathbf{q}^*$. Quasidegenerate states at $\mathbf{K} = (6, 3), (6, 6)$ show similar $S_0(\mathbf{q})$ and $G(\mathbf{r})$. In Fig. 5, we also observe a clear presence of nearly degenerate first-excited states formed by the lowest energy states at $\mathbf{K} = (5, 1), (5, 2), (5, 4), (5, 5)$. They are created from the quasidegenerate ground states by vectors $\mathbf{e}_1 = (1, 1), \mathbf{e}_2 = (-1, 1)$. A part of a less clear array of nearly degenerate second-excited states in Fig. 5 is also generated from the first-excited states by these vectors. Some other excited states in the second-excited array have the quantum numbers generated from $(1, 0)(-1, 0)$. The appearance of clearly separated low-energy bands is accounted for by low-energy particle-hole excitations in which a boson is moved from one stripe to another. These bands are almost flat, showing that such a hopping of the bosons between stripes is strongly suppressed. This band structure gives evidence of the stripe state. The band for excited states is not clear in Fig. 3 for $N = 10$. For $N = 12$, the stripe state with three stripes appears in the region $a/b = 0.4 \sim 0.65$. At $a/b = 0.5$, we confirm that these states persist for $\alpha = 0.5 \sim 0.8$. Similarly, we observe quasidegenerate ground states forming two stripes lying parallel to the y-direction in the region $a/b = 0.7 \sim 1.0$. For α beyond 0.6 at $a/b = 0.7 \sim 1.0$, quasidegenerate ground states persist to be present but their ordering is different from stripes (see below).

Let us next turn to the region of larger dipole moment. In Fig. 7, we present the energy spectrum for $N = 10$ at $\alpha = 1.0$, $a/b = 0.8$. There are several quasidegenerate states whose locations in the reciprocal space form a lattice. This means that these states have a tendency to form a bubble state. The primitive vectors are $\mathbf{e}_1$ and $\mathbf{e}_2$. Let N_b be the number of bubbles per the unit cell. As derived in Ref.[22], the relation $N_b N_D = N^2$ gives the number of bosons in a bubble $M = N/N_b = N_D/N$. In this case, $N = 10$ and $N_D = 50$, which gives $N_b = 2$ and $M = 5$. In Fig. 7, one also sees quasidegenerate first-excited levels above the quasidegenerate ground states. A part of their quantum numbers are generated by vectors $(\pm 1, 0), (0, \pm 1)$ from those of the quasidegenerate ground states. The rest of them is the first-excited state at $\mathbf{K}$ where the quasidegenerate ground states appear. These almost flat bands are accounted for by low-energy particle-hole excitations in which a boson is moved from one bubble to another. In Fig. 8, we show the pair distribution function $G(\mathbf{r})$ at $\mathbf{K} = (0, 5)$. There are two peaks at $\mathbf{r} = (0, 0)$ and $\mathbf{r} = (a/2, b/2)$, which is consistent with

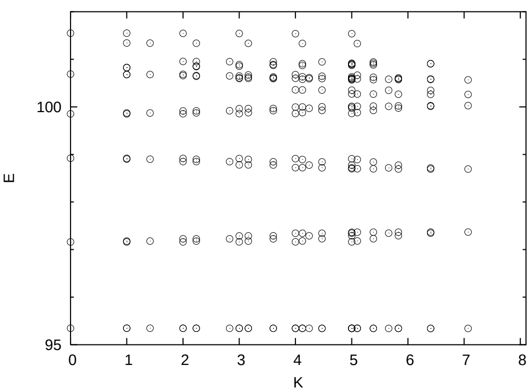

FIG. 9: Energy spectrum of the dipolar model for $N = 10$ at $\alpha = 3.0, a/b = 0.8$. Every lowest energy state in the reciprocal space is quasidegenerate.

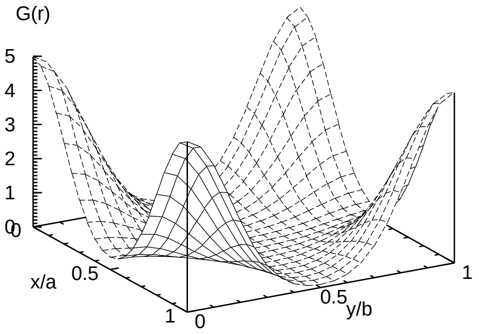

FIG. 10: $G(\mathbf{r})$ of the ground state of the dipolar model for $N = 10$ at $\alpha = 3.0, a/b = 0.8, \mathbf{K} = (0, 5)$.

the number of N_b. $G(\mathbf{r})$ for other quasidegenerate states is similar. These give evidence that these quasidegenerate states form a bubble state. The transition from the stripe state to the bubble state is observed around $\alpha \sim 0.8$. For $N = 8$, bubble states are seen in the region $\alpha = 0.8 \sim 2.0$, $a/b = 0.4 \sim 1.0$.

In Fig. 9, we present the energy spectrum for $N = 10$ at $\alpha = 3.0$, $a/b = 0.8$. The number of the quasidegenerate ground states increases compared to the $\alpha = 1.0$ case. The lowest states for every $\mathbf{K}$ become quasidegenerate. A clear presence of the band structure in Fig. 9 is readily interpreted by low-energy particle-hole excitations. These give evidence of a bubble state. In this case, $N_b = 1$ and $M = 10$. In Fig. 10, $G(\mathbf{r})$ of the lowest energy state at $\mathbf{K} = (0, 5)$ is presented. The density concentrates near the corner of the unit cell, which is consistent with $N_b = 1$. Thus, the bubble state observed here is different from the bubble state for lower α. The transition between these bubble states occurs around $\alpha \sim 2.0$ for $N = 8, 10$.

As seen above, after the collapse of the incompressible liquid, ground states are not separated from excited states by a gap. This is characteristic of a compressible state. In general, its property is sensitive to geometry (the aspect ratio). Therefore we vary the aspect ratio for values of α and study the dependence of spectra on the aspect ratio. In Fig. 11, we present energy spectra for $N = 10$ at $\alpha = 0.65, 1.0, 3.0$. For $\alpha = 0.65$, changes of the level structure accompanying level crossings are seen around $a/b \sim 0.75, 0.52, 0.25$. At $\alpha = 1.0$, a structural change is seen around $a/b \sim 0.4$. At $\alpha = 3.0$, structural changes are seen around $a/b \sim 0.7, 0.55, 0.3$. Similar structural changes are observed for other N but the values of aspect ratios at which they occur depend on N. When structural changes are not sharp, intermediate states appear around these points as seen in Fig. 11.

Let us illustrate a complicated behavior at $\alpha = 0.65$ in the region $a/b = 0.5 \sim 0.7$ where one sees many level crossings as in Fig. 11(a). As an example, we present the energy spectrum for $N = 10$ at $a/b = 0.6$ in Fig. 12. The ground state appears at $\mathbf{K} = (5, 5)$. The locations of quasidegenerate states in the reciprocal space do not form any lattice. For $N = 12$, similar states appear in the region of high aspect ratios $a/b = 0.65 \sim 1.0$ around $\alpha = 0.65$. We interpret them as intermediate states between stripe states and bubble states due to finite-size effects. The region for which such intermediate states appear should shrink as N gets large.

Let us next turn to the highly anisotropic region (a/b below 0.5) of Fig. 11(a). Energy spectrum and $G(\mathbf{r})$ shows that stripe states appear in the region $a/b = 0.25 \sim 0.5$. The quasidegenerate states in this region form a stripe state with three stripes lying parallel to the x-direction[25].

Let us next illustrate some details of the level structure for $\alpha = 1.0$ shown in Fig. 11(b). The level structure of the region $a/b = 0.2 \sim 0.4$ is different from those for the bubble state seen in the region $a/b = 0.4 \sim 1.0$. The level structure of the bubble state in the region $a/b = 0.4 \sim 1.0$ persists for $\alpha = 0.8 \sim 2.2$. As seen in Fig.11(b), it disappears around $a/b = 0.4$ and changes to that of a stripe state. For other α's, this structural change occurs around $a/b = 0.4 \sim 0.5$. The direction of stripes is parallel to the x-direction.

In Fig. 11(c), we present energy spectra versus the aspect ratio for $N = 10$ at $\alpha = 3.0$. It shows a change of the level structure around $a/b \sim 0.7, 0.54$. The bubble states disappear for lower aspect ratios. Stripe states appear at a/b below 0.54.

In stripe states in Fig. 11(a),(b),(c) at the highly anisotropic region, the direction of stripes is always parallel to the x-direction (the shorter axis). The number of stripes depends on N, α, and a/b.

Let us next turn to the region of extremely low aspect ratios below 0.2. In this region, some strange behaviors are observed. For $N = 8, 10$, the overlap of quasidegenerate ground states at $\alpha = 0$ with the Pfaffian states is large only for one sector of $\mathbf{K}$. It drops rapidly when we move to $\alpha \neq 0$ but the other two sectors for quasidegenerate ground states begin to have a large overlap with the Pfaffian states. The collapse of these two states occurs at much higher value of α than for nonextreme aspect ra-

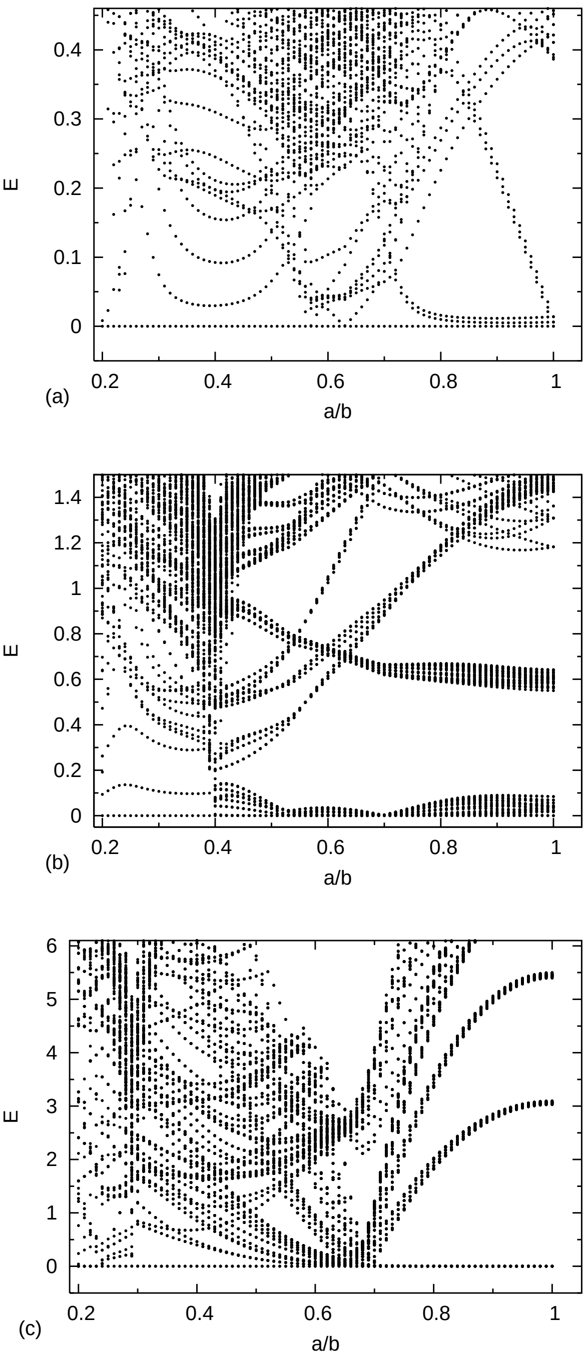

FIG. 11: Energy levels versus the aspect ratio a/b for $N = 10$. (a)$\alpha = 0.65$, (b)$\alpha = 1.0$, (c)$\alpha = 3.0$.

tios. In this region, the shapes of $S_0(\mathbf{q})$ and $G(\mathbf{r})$ for the Pfaffian states are quite similar to those of stripe states. They cannot be distinguished from a stripe state with four stripes ($N = 8$), five stripes ($N = 10$) lying parallel to the x-direction[26].

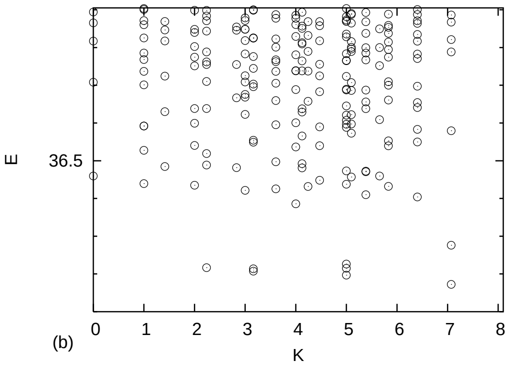

FIG. 12: Energy spectrum of the dipolar model for $N = 10$ at $\alpha = 0.65, a/b = 0.6$.

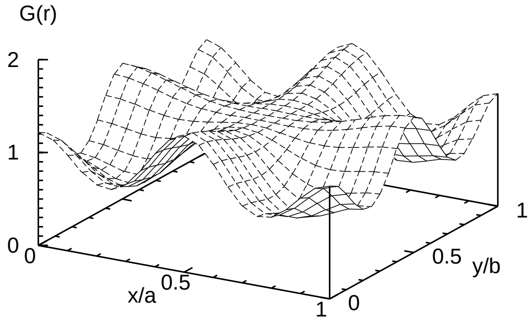

FIG. 13: $G(\mathbf{r})$ of the ground state of the dipolar model for $N = 12, \alpha = 0.6, a/b = 1.0$ at $\mathbf{K} = (6, 6)$.

Let us next present results for the isotropic case $a/b = 1.0$ where geometric symmetry is enhanced. Also for this case, two stripe states appear for $N = 10$ in the region $\alpha = 0.4 \sim 0.8$. States at $\mathbf{K} = (K_1, K_2)$ and $\mathbf{K} = (K_2, K_1)$ are exactly degenerate due to geometrical symmetry present at $a/b = 1.0$. The ground states appear at $\mathbf{K} = (0, 5)$ and $\mathbf{K} = (5, 0)$. States at $\mathbf{K} = (1, 0), (3, 0), (5, 0), (0, 1), (0, 3), (0, 5)$ are quasidegenerate and separated from the rest of the spectrum. The states at $\mathbf{K} = (1, 0), (3, 0), (5, 0)$ form two stripes parallel to the y-direction while the states at $\mathbf{K} = (0, 1), (0, 3), (0, 5)$ form two stripes parallel to the x-direction. Thus the ground state at $a/b = 1.0$ is a linear combination of these two stripe states. Similarly the ground state at $\mathbf{K} = (6, 6)$ for $N = 12$ is not a stripe state with a broken translational symmetry for one direction, nor a bubble state with a broken translational symmetry for two directions. In Fig. 13, we present $G(\mathbf{r})$ of the ground state at $\alpha = 0.6, \mathbf{K} = (6, 6)$. They indicate that the ground state has a strong density-density correlation along two stripes lying parallel to the x- and y-directions. We observe that this shape of $G(\mathbf{r})$ at $a/b = 1.0$ persists for $N = 10, \alpha = 0.4 \sim 0.8$.

Near the isotropic case, one expects that there may be a competence between stripe states with perpendicular directions. This is actually the case for $N = 10$ in a region around $a/b \sim 0.8$. The direction of the stripes

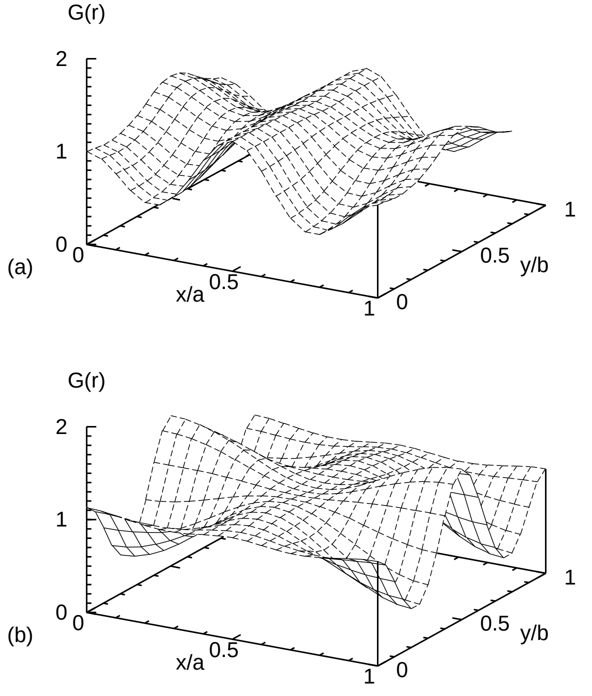

FIG. 14: $G(\mathbf{r})$ of various ground states of the dipolar model. (a) $N = 10, \alpha = 0.49, \mathbf{K} = (5, 0)$. (b) $N = 10, \alpha = 0.50, \mathbf{K} = (0, 5)$.

changes as one varies α. There is a level crossing at $\alpha \sim 0.496$ for $a/b = 0.8$. In the region $\alpha < 0.496$, the ground state appears at $\mathbf{K} = (5, 0)$. At $\alpha \sim 0.496$, the lowest energy states at $\mathbf{K} = (5, 0)$ and $\mathbf{K} = (0, 5)$ are quasidegenerate. In the region $\alpha > 0.496$, the ground state appears at $\mathbf{K} = (0, 5)$. We present $G(\mathbf{r})$ of the ground states for $\alpha = 0.49, 0.50$ in Fig. 14 (a),(b). In the region with $\alpha < 0.496$, the quasidegenerate ground states at $\mathbf{K} = (5, 0), (3, 0), (1, 0)$ form a stripe state with two stripes lying parallel to the y-direction. At $\alpha = 0.50$, the ground state at $\mathbf{K} = (0, 5)$ is an intermediate state between two stripes with perpendicular directions. At $\alpha = 0.65$, the stripe state with two stripes lying parallel to the x-direction appears.

Before ending this section, let us briefly discuss the V_0-V_2 model. Previously the collapse of the incompressible liquid for the two-body contact interaction V_0 by the V_2 interaction has been observed in the spherical geometry[19,20]. In Fig. 1, we present the squared overlaps of two degenerate ground states and a nearly degenerate state with the Pfaffian states for $N = 10$ at $a/b = 1.0$. As in the case of the dipolar interaction, a moderate V_2 interaction stabilizes the Pfaffian state. It collapses around $\alpha \sim 0.25$ as seen in Fig. 1. We confirm that quasidegenerate ground states with a tendency to form stripes appear after the collapse. When we further increase α, two kinds of quasidegenerate ground states with characteristics to form bubbles appear as in the case of the dipolar model.

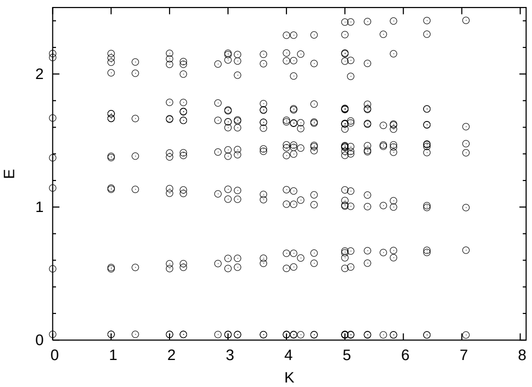

FIG. 15: Energy spectrum of the V_2 model for $N = 10$ at $a/b = 0.8$.

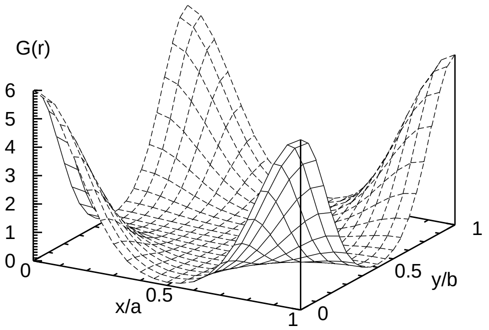

FIG. 16: $G(\mathbf{r})$ of the ground state of the V_2 model for $N = 12$ at $a/b = 1.0, \mathbf{K} = (6, 6)$.

IV. RESULTS FOR THE V_2 MODEL

In this section, we present results for the V_2 model. We present the energy spectrum for $N = 10$ at $a/b = 0.8$ in Fig. 15. The lowest energy states at every point in the reciprocal space are quasidegenerate and separated from the rest of the spectrum. Also, in Fig. 15, several flat excited bands are clearly seen. It is consistent with the presence of low-energy particle-hole excitations. These observations give evidence of a tendency to the formation of a bubble state. The pair distribution function $G(\mathbf{r})$ of quasidegenerate states are similar to those of the bubble states of the dipolar mode at $\alpha = 3.0$. Similar shapes of $G(\mathbf{r})$ are observed for $N = 8, 12$ at $a/b = 0.8 \sim 1.0$. Fig. 16 shows $G(\mathbf{r})$ for $N = 12, a/b = 1.0$.

We present energy spectra versus the aspect ratio for $N = 10$ in Fig. 17. The spectral flow of the V_2 model is similar to that of the dipolar model at α above 2.0. As seen in Fig. 17, quasidegenerate ground states forming a bubble state persist for $a/b = 0.5 \sim 1.0$. The level structure changes to that of a stripe state around $a/b =$

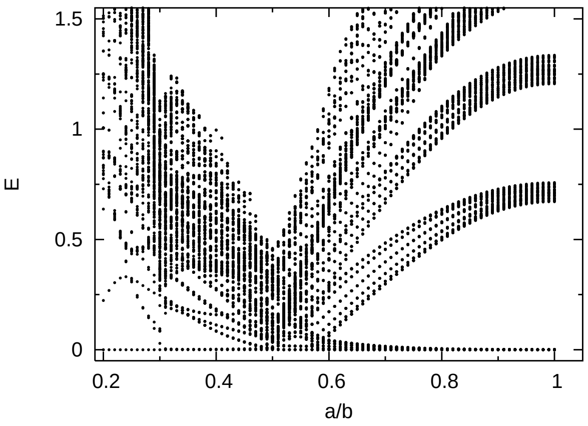

FIG. 17: Energy levels versus the aspect ratio of the V_2 model for $N = 10$.

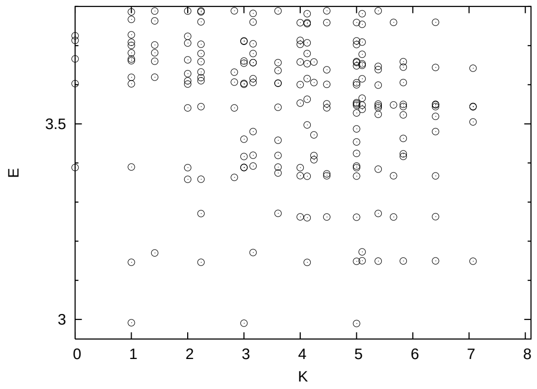

FIG. 18: Energy spectrum of the V_2 model for $N = 10$ at $a/b = 0.35$. The ground state at $\mathbf{K} = (0, 5)$ and states at $\mathbf{K} = (0, 3), (0, 1)$ are quasidegenerate.

0.45. Fig. 18 shows the energy spectrum at $a/b = 0.35$. The ground state at $\mathbf{K} = (0, 5)$ and the lowest energy states at $\mathbf{K} = (0, 3), (0, 1)$ are quasidegenerate. In Fig. 18, clearly separated low-lying bands are seen, which is consistent with the existence of particle-hole excitations of a stripe state. The direction of stripes is always parallel to the x-direction.

Fig.19 shows the overlap of the ground state of the dipolar model with the ground state of the V_2 model. The overlap is close to 1.0 for α beyond $\sim$ 2.2. In the pseudopotential expansion, the dipolar model has higher order terms beyond V_2 but this result suggests that, for aspect ratios above $\sim$ 0.5, quasidegenerate ground states for the dipolar model at large α coincide with those of the V_2 model.

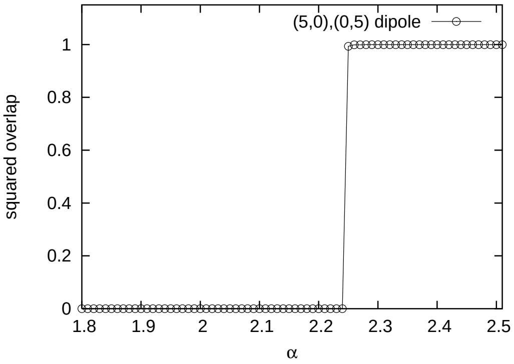

FIG. 19: The squared overlaps of the two degenerate ground states of the dipolar model with the ground states of the V_2 model are shown for $N = 10$ at $a/b = 1.0$. We present results for the two ground states at $\mathbf{K} = (5, 0), (0, 5)$. $\mathbf{K} = (0, 5)$ and $\mathbf{K} = (5, 0)$ are exactly degenerate due to geometrical symmetry at $a/b = 1.0$.

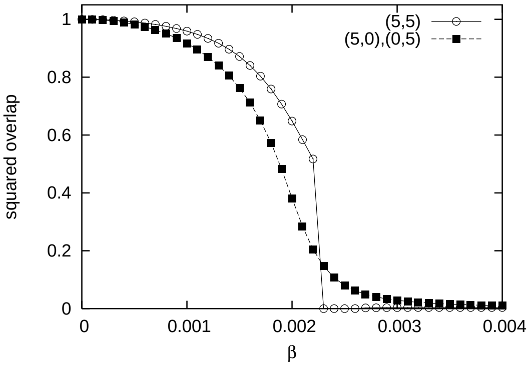

FIG. 20: The squared overlaps of the two degenerate ground states and a nearly degenerate state for the $V_{3\mathrm{b}} + V_2$ model with the Pfaffian states are shown for $N = 10$ at $a/b = 1.0$. The Pfaffian states exist at $\mathbf{K} = (5, 5), (5, 0), (0, 5)$. The two ground states of the $V_{3\mathrm{b}} + V_2$ model appear at $\mathbf{K} = (5, 0), (0, 5)$. $\mathbf{K} = (0, 5)$ and $\mathbf{K} = (5, 0)$ are exactly degenerate due to geometrical symmetry at $a/b = 1.0$.

V. RESULTS FOR THE THREE-BODY INTERACTION

In this section, we present results for the $V_{3\mathrm{b}} + V_2$ model. We set $\beta \equiv V_2/C_{3b}$. We add a moderate V_2 interaction (small β) and examine the stability of the Pfaffian states which are the exact zero-energy ground states at $\beta = 0$. In Fig. 20, we show the squared overlaps of nearly degenerate ground states at $a/b = 1.0$ with the Pfaffian states at each $\mathbf{K}$ where Pfaffian states exist. The overlaps decrease monotonically as β increases. The overlaps drop around $\beta \sim 2.0 \times 10^{-3}$. The collapse is not as sharp as that of the dipolar model. For other aspect ratios we have investigated, this collapse always occurs. The value of β where this collapse occurs increases as a/b decreases.

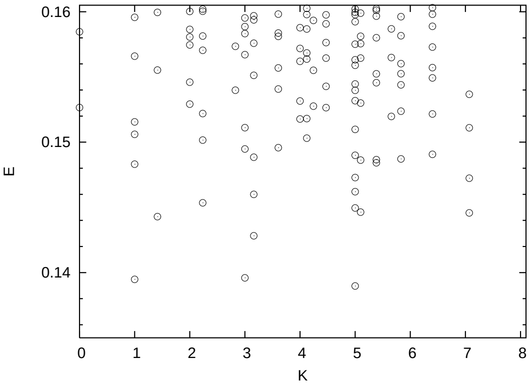

FIG. 21: Energy spectrum of the $V_{3b} + V_2$ model for $N = 10$ at $\beta = 1.0 \times 10^{-2}, a/b = 0.8$. The ground state at $\mathbf{K} = (0, 5)$ and states at $\mathbf{K} = (0, 1), (0, 3)$ are quasidegenerate.

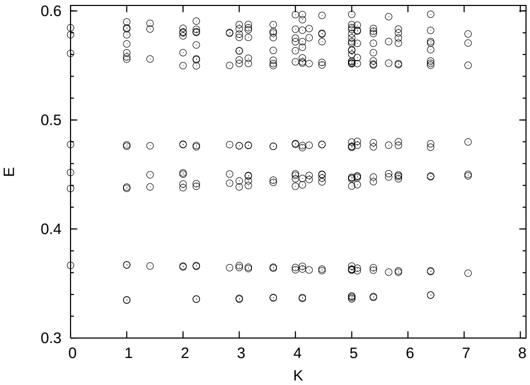

FIG. 22: Energy spectrum of the $V_{3b} + V_2$ model for $N = 10$ at $\beta = 0.1, a/b = 0.8$. The quasidegenerate states are at $\mathbf{K}$ =(1,0),(0,1),(2,1),(1,2)(3,0),(0,3),(2,3),(3,2) ,(4,1),(1,4),(4,3),(3,4),(5,0),(0,5),(4,5),(5,4),(2,5),(5,2).

Let us next turn to states after the collapse. At high aspect ratios, we observe quasidegenerate ground states forming stripes. The stripe state changes to a bubble state around $\beta \sim 2.5 \times 10^{-2}$. As we further increase β, the ground state starts to have a large overlap with the ground state of the V_2 model at β above 1.0. The structure of the energy spectrum is similar to that of the V_2 model.

As an example of high aspect ratios, we present the energy spectrum for $N = 10$ at $a/b = 0.8, \beta = 1.0 \times 10^{-2}$ in Fig. 21. The ground state at $\mathbf{K} = (0, 5)$ and states at $\mathbf{K} = (0, 3), (0, 1)$ are quasidegenerate. These states form a stripe state. The direction of stripes is parallel to the x-direction and the number of stripes is two while first-excited levels are not clearly separated in Fig. 21. The pair distribution function $G(\mathbf{r})$ for the ground state at $\mathbf{K} = (0, 5)$ is similar to that of the stripe state of the dipolar model presented in Fig. 4. When we decrease the aspect ratio, the stripe state changes to an intermediate state at $a/b \sim 0.5$. If we further decrease the aspect ratio, a stripe state reappear at a/b below 0.3.

A bubble state appears at high aspect ratios for $\beta = 0.025 \sim 1.0$. In Fig. 22, we present the energy spectrum for $N = 10$ at $\beta = 0.1, a/b = 0.8$. There are quasidegenerate ground states arrayed in the lattice with the primitive vectors $\mathbf{e}_1$ and $\mathbf{e}_2$, indicating a formation of bubbles. The presence of clearly separated bands in Fig. 22 gives further evidence of it. The $G(\mathbf{r})$ of quasidegenerate states is similar to that of the bubble state of the dipolar model presented in Fig. 8. At low aspect ratios a/b below 0.3, the quasidegenerate ground states remain to form a stripe state. The direction of stripes is always parallel to the x-direction. The number of stripes varies for N and a/b. Intermediate states appear in the region $a/b = 0.3 \sim 0.5$.

VI. CONCLUSIONS

We have exhibited evidence that bosons with a dipole moment in the lowest Landau level at $\nu = 1$ have phases of incompressible liquid, stripes and bubbles based on exact diagonalizations up to $N = 12$. While a moderate amount of the dipolar interaction stabilizes the incompressible liquid, a further amount induces a collapse of it. The state after the collapse is a compressible state. Up to $N = 12$, it is a stripe state or an intermediate state between stripes and bubbles. The number and the direction of stripes are sensitive to the aspect ratio, the strength of the interaction and the number of particles. As the dipolar interaction gets strong, two kinds of bubble states appear for high aspect ratios. The transition between them is observed as the dipolar interaction gets strong. On the other hand, for small aspect ratios, stripe states remain to appear even when the dipolar interaction is rather strong.

We have also considered the V_2 model where the bosons do not have a hard-core. It has turned out that it does not have a phase of incompressible liquid. Its ground state is a bubble state for aspect ratios above 0.5. A certain amount of the V_0 interaction induces a transition to another bubble state a different array. We have observed that, for high aspect ratios, the quasidegenerate ground states for the dipolar interaction at the strong limit have large overlaps with those of the V_2 model. For low aspect ratios below 0.5, quasidegenerate ground states of the V_2 model are identified to be a stripe state.

We have also studied the model where the bosons interact through the three-body contact interaction for which the Pfaffian state is the exact ground state. It shows similar properties as those of the dipolar model : our results give evidence that the model has phases of stripes and bubbles.

Finally we remark that the geometry treated in this paper is a subset of the general geometry of torus where the period vectors are not necessarily perpendicular.

Acknowledgment. A part of numerical calculations has been performed at the supercomputing facility of Institute for Solid State Physics, Univ.of Tokyo. K.I. is partially supported by Grant-in-Aid for Science Promotion and also by the SAKURA project organized by JSPS and CNRS.

Note Added. While we were completing this work, a preprint which has a partial overlap with this paper appeared[27]. Energy levels which show degenerate ground states which are characteristic of the Pfaffian and stripes are observed at a strength of the dipolar interaction.

---

[1] K. W. Madison, F. Chevy, W. Wohlleben, and J. Dalibard, Phys. Rev. Lett. 84, 806 (2000).

[2] J. R. Abo-Shaeer, C. Raman, J. M. Vogels, and W. Ketterle, Science **292**, 476 (2001).

[3] N. R. Cooper, N. K. Wilkin, and J. M. F. Gunn, Phys. Rev. Lett. **87**, 120405 (2001).

[4] N. K. Wilkin and J. M. F.Gunn, Phys.Rev.Lett. **84**, 6 (2000).

[5] N. K. Wilkin, J. M. F. Gunn, and R. A. Smith, Phys.Rev.Lett. **80**, 265 (1998).

[6] R. B. Laughlin, Phys. Rev. Lett. **50**, 1395 (1983).

[7] G. Moore and N. Read, Nucl. Phys. **B360**, 362 (1991).

[8] R. Morf, Phys. Rev. Lett. **80**, 1505 (1998).

[9] S. Das Sarma, M. Freedman, C. Nayak, Phys. Rev. Lett. **94**, 166802 (2005).

[10] F. Dalfovo, S. Giorgini, and L. P. Pitaevskii, Rev. Mod. Phys. **71**, 463 (1999).

[11] A. Griesmaier, J. Werner, S. Hensler, J. Stuhler, and T. Pfau, Phys. Rev. Lett. **94**, 160401 (2005).

[12] N. R. Cooper, E. H. Rezayi, and S. H. Simon, Phys. Rev. Lett. **95**, 20042 (2005).

[13] E. H. Rezayi, N. Read, and N. R. Cooper, Phys. Rev. Lett. **95**, 160404 (2005).

[14] N. R. Cooper and E. H. Rezayi, Phys. Rev. A **75**, 013627 (2007).

[15] F. D. M. Haldane, Phys. Rev. Lett. **51**, 605 (1983).

[16] M. Greiter, X. G. Wen, and F. Wilczek, Phys. Rev. Lett. **66**, 3205 (1991); Nucl. Phys. **B374**, 567 (1992).

[17] K. Ino, Nucl. Phys. **B532**,782(1998).

[18] F. D. M. Haldane, Phys. Rev. Lett. **55**, 2095 (1985).

[19] N. Regnault and T. Jolicoeur, Phys. Rev. Lett. **91**, 030402 (2003); Phys. Rev. B **69**, 235309 (2004).

[20] N. Regnault and T. Jolicoeur, eprint cond-mat/0601550.

[21] E. H. Rezayi, F. D. M. Haldane, and K. Yang, Phys. Rev. Lett. **83**, 1219 (1999).

[22] F. D. M. Haldane, E. H. Rezayi, and K. Yang, Phys. Rev. Lett. **85**, 5396 (2000).

[23] A.A. Koulakov, M.M. Fogler, and B.I. Shklovskii, Phys. Rev. Lett. **76**,499 (1996) ; M.M.Fogler, A.A. Koulakov, and B. I.Shklovskii, Phys. Rev. B **54**,1853(1996).

[24] F. D. M. Haldane, Chap. 8 in *The Quantum Hall Effect*, edited by R. E. Prange and S. M. Girvin, 2nd ed. (Springer-Verlag, Berlin, 1990).

[25] For $N = 8$, a stripe state with three stripes does not appear.

[26] A similar modulation of the Laughlin state for fermions in extremely anisotropic geometry is mentioned in Ref.[24].

[27] B. Chung and T. Jolicoeur, eprint cond-mat/07123185.